

UC Merced

UC Merced Previously Published Works

Title

Potential of Balloon Photogrammetry for Spatially Continuous Snow Depth Measurements

Permalink

<https://escholarship.org/uc/item/3rd949v7>

Journal

IEEE Geoscience and Remote Sensing Letters, 17(10)

ISSN

1545-598X

Authors

Li, Dongyue
Wigmore, Oliver
Durand, Michael T
et al.

Publication Date

2020-10-01

DOI

10.1109/lgrs.2019.2953481

Peer reviewed

Potential of balloon photogrammetry for spatially continuous snow depth measurements

Dongyue Li, Oliver Wigmore, Michael Durand, Benjamin Vander-Jagt, Steven A. Margulis, Noah Molotch, Roger Bales

Abstract — We carried out two aerial surveys using a weather balloon as the platform to measure the snow depth in the Wolverton watershed, CA: one when the site was snow covered and the other one after the snow melted out. We reconstructed the 3D surfaces of the site using structure-from-motion (SfM) photogrammetry of the photos taken in the surveys, and differenced the heights of the two surfaces to obtain the snow depth. The snow depth estimates corresponded well with 32 manual measurements of snow depth, with $R=0.87$ ($p<0.05$) and a RMSE of 7.6 cm, the majority of which is a 6 cm systematic bias due to vegetation rebound in the snow-off measurements. The relative depth error is 17% in the extremely dry year of sampling (i.e. 2015), and is expected to decrease for deeper snow because the absolute error of SfM is relatively static. The processed snow depth is able to capture the snow spatial variability at sub-meter scale. This study suggests that balloon photogrammetry is a repeatable, flexible, economical, and safe method for continuous snow depth measurement at small scales, and could complement existing remote sensing platforms (e.g. aircrafts, satellites, drones) for snow observations in open areas by providing spatial continuity, long observation time, and customizable resolution.

Index Terms — snow, balloon remote sensing, photogrammetry

I. INTRODUCTION

Seasonal snowmelt is a major source of water on which over a billion people worldwide depend. In the northern hemisphere, more than half of the terrestrial water cycle is dominated by snow [1]. Thus, accurate estimation of snow depth and snow water equivalent (SWE) is critical to water management in snow-dominated watersheds. In-situ snow measurements have a long history of being applied for statistically based forecasting of snowmelt runoff, but they are spatially sparse and thus are unrepresentative of the spatial variability and the total volume of SWE [2]. Modeling and remote sensing are two primary ways in which the spatial variability of SWE can be estimated. However, large-scale SWE estimates from these two methods often have errors and uncertainties as a result of a number of reasons [3], including our limited understanding of the physical snow processes and the complex interactions among snow, terrain, and other landscape attributes (e.g. vegetation) [4]. Snow-focused field experiments (e.g. SnowEx [5]), and long-term field laboratories (e.g. the Critical Zone Observatories) have produced comprehensive measurements of meteorological conditions, vegetation, soil properties, and snow conditions at catchment or smaller scales. These intensive measurements have revealed key connections between snow and ecosystems within relatively small areas, providing a basis for advancing the understanding of the physical processes at larger scales [5]. However, even at small scales, snow depth, which is one of the most fundamental variables in snow hydrology, has been measured almost entirely at the point scale; the collection of dense snow sampling (e.g. snow transects in SnowEx) is limited by tremendous labor and logistical demands. A method that can continuously measure snow depth with minimal human intervention would be most valuable in this context.

Spaceborne and airborne remote sensing provide spatially continuous snow observations [6], but these

platforms are limited by high cost and lack of flexibility. Drones are attractive for Earth observation because of their flexibility, cost-efficiency, and the fact that they can bridge the scale gap between in-situ measurements and spaceborne and airborne remote sensing observations [7]. However, the major hurdles for the wide adoption of drone observations include relatively short flight times (mostly less than an hour) and regionally dependent regulations that restrict drone flights. For example, drone flights (launching and landing) in the U.S. are prohibited or heavily restricted on all lands in the National Parks and over half of the National Forest lands designated as Wilderness Areas [8,9]; these include much of the mountains in the western U.S. where seasonal snow cover is a critical water resource. While flight permits may be granted for research activities on a case by case basis, for snow research, the ideal timing for observations may not be realized due to the rapid snow accumulation and ablation processes and the time needed for permit approval. In this context, a non-restricted method that shares the similar characteristics with drones is attractive.

Weather balloons are desirable complements of current ground observations and remote sensing platforms with respect to spatial resolution, temporal duration, and spatial coverage [10]. Balloons have several unique attractions. First, weather balloons are not restricted for safety or ecological concerns and can be flexibly deployed virtually anywhere [11]. Second, compared with aircraft and satellites, weather balloons have much lower cost and wider accessibility. Third, balloons can easily change flight height for user-preferred spatial resolution and extent, and can also hover above an area for continuous measurements over several days. Fourth, balloons constantly sway when aloft, generating random sensor orientations and altitudes that can mitigate the systematic errors in photogrammetric processing that originate from regular flight patterns, which particularly plague drone surveys

[12]. In recent years, miniaturization has resulted in advanced sensors at various spectral bands compatible with balloons, such as multi-spectral radiometers [12], LiDAR [13], and hyper-spectral imagers [14]. The flexibility, versatility, and cost-efficiency of balloon-based remote sensing have promoted its usage in both traditional (e.g. [15]) and unconventional (e.g. [16]) remote sensing applications. To our knowledge, however, balloons have not been used as platforms for snow measurements.

In this letter, we describe a snow depth mapping study using the structure-from-motion (SfM) photogrammetry [17] and the aerial images taken from balloon aerial snow surveys. We also discuss the potentials and limits of balloon photogrammetry in continuous snow depth estimation at small scales.

II. STUDY AREA

We conducted our study at the Wolverton Meadow (118.737W, 36.590N, Fig 1) located close to the Wolverton Recreation Area of Sequoia National Park. The elongated meadow is oriented north-south, with hills surrounding its south, east and west sides. Snowmelt from the hillslopes above the meadow converges to a creek at the center of the meadow that flows into the Marble Fork of the Kaweah River from the north end of the meadow. The meadow is about 1100 m long, 100 m wide, and 2300 m above sea level. Peak snow accumulation often exceeds 2 m in a year with average winter precipitation, and snowmelt makes up ~70% of the local runoff [18]. The meadow is grass-covered and the surrounding hills are mixed-conifer forested with trees over 40 m tall. Our snow survey focused on the north half of the meadow.

III. METHODS

A. Aerial photography system

The aerial photography system (Fig 2) included a 7ft PVC weather balloon filled with helium and a suspended camera rig. The balloon provided ~2.5 kg of lift and was tethered to the ground with 350 m of 330 lb paracord. In light winds the balloon remained almost directly overhead, and could be moved around the domain. A modified kite aerial photography rig [19] was attached to the tether line to hold the camera. The rig was custom built from aluminium and carbon fibre and was tied to the tether line with a picavet cross system, which helped maintain nadir camera orientation. The rig is able to hold up to three cameras simultaneously for multi-spectral measurement; we fit the rig with a single Canon Powershot S110 camera to capture images in the visible spectrum for this study. This camera is small, lightweight, relatively low-cost and allows full manual control of all imaging parameters such as F-stop, ISO, and exposure length. The camera was automatically triggered when it is aloft using a Canon Hack Development Kit, which is open-source firmware that allows various camera functions to be controlled with custom scripts. We used the `drone.bas` script [20] to set the shutter to be automatically triggered every 10 seconds. We attached a consumer grade GPS (i-gotU GT120) to the rig to record a 1Hz track log of the

camera position. Individual images could then be geotagged based on the photo time stamp.

B. Ground and aerial measurements

We completed the snow-on surveys on March 2, 2015 and the snow-off survey on April 29, 2015. Before each aerial survey, we installed 13 highly visible ground targets across the study site as ground control points (GCP), which control the overall accuracy of the photogrammetry processing and thus need to be measured with high accuracy. GCPs positions were surveyed with a Topcon GRS 1 L1 GNSS receiver and Topcon PG-A1 antenna rover system. Each position was occupied for 5 minutes at 1 Hz intervals using the Post-Processed Stop-and-Go (PPSG) method. Additionally, a local base station (Topcon Hiper SR L1/L2) was installed in the meadow and collected 1Hz observations for approximately 3 days; the base station itself was precisely positioned using the Natural Resources Canada online Precise Point Positioning tool to 0.001m accuracy. Rover positions were post-processed relative to the local base station for higher accuracy using Topcon Magnet Tools; all final GCP positions were within an error range of 0.001 m to 0.01 m.

Following the GCP survey, we sent the balloon aloft for aerial mapping. We conducted the snow-on aerial survey between 10:30 am and 2:00 pm PST, when around 1200 aerial photos were taken in overcast weather with relatively low solar illumination and wind speeds up to 4.5 m/s. The snow-off aerial survey was carried out from 9:00 am to 11:00 am PDT with around 700 aerial photos collected on a warm sunny day with almost no wind. For both surveys we flew the balloon at ~60m above ground level (agl), although some variation occurred due to changes in tether angle. This was the minimum safe altitude to keep the balloon clear of tall trees within the study area. The camera rig was suspended roughly 15 m below the balloon (~45 m agl) to minimize the potential effects of sudden balloon movements on camera stability (Fig 2b and 2c). This resulted in a horizontal ground resolution of about 1.4 cm. A ground operator dragged the tether and walked across the survey region until all locations were sufficiently photographed. We took many more photos than necessary in the surveys to allow blurry and/or poorly exposed images to be deleted and to guarantee the remaining high-quality photos had sufficient overlap (>90%). The camera was set to favor a fast shutter speed (>1/1000s) and high F-stop, which helped reduce motion blur and improve the depth of field focus. ISO was kept below 400 to minimize graininess. We intentionally under-exposed photos in the snow-on survey because the brightness of fresh snow surfaces could cause image washout and the loss of fine surface features needed for image matching in photogrammetry.

We took manual snow depth samplings at 30 points across the study area simultaneously with the snow-on aerial mapping. The position of each snow depth sampling was surveyed with the GPS rover system. We used these manual depth samplings to evaluate the snow depth retrieved from the aerial

surveys. We also made two snow balls (of approximate diameter of 0.5 meter and 1 meter, respectively) and measured the altitude of the top of them to attempt to assess the accuracy of the method for deeper snow, given that the natural snow accumulation was exceptionally low in water year 2015.

C. Photogrammetric processing

Photogrammetry is the basis for retrieving 3D geospatial information from 2D photographs. The details of the photogrammetric method are widely available [21], so we omit the details here for brevity. In its essence, photogrammetry reconstructs the 3D photography scene from the projective bundle geometry within a series of overlapped 2D stereo photos that cover the scene (space re-section), and calculates the 3D coordinate of the objects within the scene (surface reconstruction). It then minimizes the overall error of the 3D reconstruction with respect to the measured GCPs (error adjustment). Such processing, initially done with analytical instruments, has been fully digitalized in the computer era, forming the basis of digital photogrammetry. The SfM used in this study is a modern form of digital photogrammetry. Traditional photogrammetry relies on dedicated and expensive aerial cameras with known internal geometry, and typically a small number of photos are collected and processed in each survey. In comparison, SfM uses several hundreds or thousands of images collected with inexpensive and lower-quality sensors and is able to recreate 3D models in a highly automated process, which significantly widens the utility and accessibility of photogrammetry. These characteristics of SfM are made possible by more robust image matching, error adjustment, and more powerful computing. SfM is a proven method that has been widely used in environmental monitoring [e.g. 7, 19, 22]. We used Agisoft Photoscan Professional for the SfM processing; this software has been widely used and reported in the literature, e.g. [19]. In both the snow-on survey and the snow-off survey processing, we quality controlled the aerial images and manually marked the GCPs on them. The software was then able to generate sparse and dense point clouds, followed by 5 cm horizontal resolution orthomosaics and finally the 10 cm resolution Digital Surface Model (DSM). We estimated snow depth through subtraction of the snow-off DSM from the snow-on DSM, also at 10 cm spatial resolution.

IV. RESULTS AND DISCUSSION

A. Aerial survey results

Fig 3 shows the study site and example aerial photos from the snow-on and snow-off surveys. Generally, the high spatial resolution aerial photos (1.4 cm) capture the details of the snow and ground features. For example, trails and footprints on the snow (Fig 3a, 3c) and the texture of the grass (Fig 3b, 3d) are clearly observable. Grasses had emerged over much of the meadow by the time of the snow-off survey, especially along the sides of the creek (Fig 3d).

B. Snow depth estimates from photogrammetry

Most of the ground in the mapping area was covered by snow with depths around 30 cm (Fig 4a). The high-resolution SfM snow depth estimate characterizes the fine details of the snow distribution, including the sled tracks on the tobogganing hills in the Wolverton recreational site (Fig 4b), the trails that tourists made to access different parts of the recreational area (Fig 4d), and the two snow balls we made for deep snow estimate (at the lower left corner of Fig 4b). The details of the creek meander and the patchy snow on the river bank (Fig 4c), and the extent of the ponds (Fig 4e) were all clearly retrieved in the DSM.

The snow depth estimate from SfM correlates well with the depth measurements at the 30 manual depth samplings and the 2 snowball measurements ($R=0.87$ with $p<0.05$, Fig 5), but is systematically low-biased by ~6 cm. The overall root mean square error (RMSE) of the snow depth estimate is about 7.6 cm across all the depth measurements, which is less than that reported in drone-based snow observation. As discussed, the major reason is the irregular motions of the balloon in the air generates random sensor orientations and altitudes, which has been demonstrated [12] to be able to mitigate the systematic orientation errors that impact the SfM processing of images taken from platforms that have a more regular flight trajectory. The bias in the snow depth estimate in this study is largely caused by two reasons. First, in the snow-on survey, the grass buried under the snowpack were withered and bent, but by the time of the snow-off survey, these buried grass had rebounded and had grown taller, which increased the surface height of the snow-off survey, and in turn generated a low-bias when subtracting the snow-off surface height from the snow-on surface height to calculate the snow depth. This bias could be mitigated in one of the following ways in future studies: 1) collecting the snow-off survey immediately after the site becomes snow free; 2) interpolating a vegetation thickness surface from a random selection of point measurements, and subtract it from the snow-off DSM; 3) where available, using an existing and verified bare earth DEM as the snow-off DSM. Second, the manual snow sampling could have positive error. The soil under the snow was soft during the snow-on survey (especially in places close to the creek), so the snow sampling probe could be pushed into the soft soil while it should be right at the soil snow interface, and thus over-measured the snow depth.

Over 90% of 32 depth sampling points had a snow depth estimate error less than 10 cm (Fig 6a), and the snow depth estimate at more than a half of all these sampling points had a relative error (defined as the ratio of the snow depth estimate error to the measured snow depth) less than 20% (Fig 6b). The mean relative error over all the sampling points was 17%. The absolute error in SfM is a combination of the errors of the surveyed GCP coordinates (negligible, as surveyed to sub-centimeter accuracy), the GCP placement error (estimated at a couple of cm), and the SfM model error; the combined errors for SfM models are typically around 5-10 cm in the vertical axis, and such absolute error of SfM is fairly static [21], i.e. in snow depth

estimates, the absolute photogrammetric depth error should not increase with snow depth increases; this is superior to some other remote sensing depth measurements whose errors increase with snow depth increases, as the signal needs to travel through the entire snowpack (e.g. passive microwave). This also suggests that the relative snow depth error in this study should decrease in a normal snow year, since 2015 was extremely dry and the base snow depth values were small. This can be demonstrated from the snow depth estimates at the two snow balls that have similar absolute depth error to the other sampling points (the two stand-out points with 61 cm and 92 cm measured depth in Fig 5), even though the snowballs have much larger depths (heights). It should be noted that a more accurate snow measurement is more important in dry years than in wet years, as the water management has less room for error in dry years.

The semivariogram in Fig 7 shows the snow depth estimate contains significant information of the snow spatial variability at the length scale of several meters, and is able to reveal the spatial variability at sub-meter scale level. The significant snow variability in this study (Fig 3a, 3c) was jointly caused by grass, snow playing, and walking in the field; while the snow variability caused by these reasons is not of the interest of hydrologic studies, these results indeed prove the capability of this new technique in revealing fine-scale snow variability, which is not immediately available from many other methods. Also, this technique should be able to capture the snow variability caused by natural reasons at similar scales.

C. Potentials and limits of balloon photogrammetry for snow depth measurement

Compared with the existing low-altitude remote sensing platforms that mostly consist of drones and crewed aircraft, balloon-borne platforms offer some key benefits: 1. There are fewer restrictions on where balloons can be deployed. 2. Balloon systems are more flexible; their deployment requires a lower technical entry bar. 3. Balloon systems can be flown safely in marginal weather conditions (e.g., rain, snow). 4. Balloon-borne images may produce more accurate DEMs as a result of random variations in the orientation and altitude of the sensor. 5. Balloon systems can be continuously deployed for days, which facilitates more frequent and longer term observations.

Balloon mapping is a potentially low-cost system, however, this depends on what components are selected. For example, a basic weather balloon can be purchased for <\$100, while a high end aerostat can cost many thousands. Similarly, suitable camera systems can be purchased for as little as \$100, or as much as \$5000. The full purchasing price of all the equipment and software used in this study is about \$3000, but options other than outright purchase are available to reduce the cost, e.g. access to the requisite GNSS survey equipment can often be procured through commercial rental, pooled university resources, or UNAVCO. SfM processing software can be obtained at a lower cost on a per-project or subscription basis, or

with discounted education licenses and open source software packages.

Measuring snow depth with balloon photogrammetry also comes with some clear limitations. First, balloon-borne data collection is limited to open areas and forest clearings, because the processed DSM heights in forested areas are only of the canopy top, rather than the snow beneath. To measure the snow under the vegetation, LiDAR is promising as it can penetrate the vegetation to some extent. Second, because the balloon must be walked across the study area, so there is a labor and logistical limit to the spatial footprint that can be effectively covered. Thus, this method is mostly suitable at scales around 2 km² for small-scale measurements.

V. CONCLUSIONS

Overall, balloon photogrammetry is a repeatable, economical, flexible, and environment-friendly method for spatially continuous estimates of snow depth at small scales. It complements the existing remote sensing and in-situ snow depth measurements in open areas by offering spatial continuity, long observation time, and customizable resolution that is able to reveal the spatial variability of snow at sub-meter scale level.

REFERENCES

- [1] Barnett, T.P., Adam, J.C. & Lettenmaier, D.P., "Potential impacts of a warming climate on water availability in snow-dominated regions". *Nature*, 438(7066), p.303. 2005
- [2] Guan, B., Molotch, N. P., Waliser, D. E., Jepsen, S. M., Painter, T. H., & Dozier, J., "Snow water equivalent in the Sierra Nevada: Blending snow sensor observations with snowmelt model simulations". *Water Resour Res*, 49(8), 5029-5046. 2013
- [3] Lettenmaier, D. P., Alsdorf, D., Dozier, J., Huffman, G. J., Pan, M., & Wood, E. F. "Inroads of remote sensing into hydrologic science during the WRR era". *Water Resour Res*, 51(9), 7309-7342. 2015
- [4] Molotch, N. P., & Bales, R. C.. SNOTEL representativeness in the Rio Grande headwaters on the basis of physiographics and remotely sensed snow cover persistence. *Hydrol Process*, 20(4), 723-739. 2006
- [5] Kim, E., "How can we find out how much snow is in the world?" *Eos*, 99, 2018.
- [6] Dozier, J. "Mountain hydrology, snow color, and the fourth paradigm". *Eos*, 92(43), 373-374. 2011
- [7] Bühler, Y., Adams, M.S., Bösch, R. and Stoffel, A., 2016. Mapping snow depth in alpine terrain with unmanned aerial systems (UASs): potential and limitations. *The Cryosphere*, 10(3), pp.1075-1088.
- [8] Policy Memorandum 14-05, "National Park Service Interim Policy on Unmanned Aircraft". https://www.nps.gov/policy/PolMemos/PM_14-05.htm, last visited: March 11th, 2019.
- [9] Drone (Unmanned Aircraft Systems) Use on National Forest Lands & the Protection of Wildlife. https://www.fs.usda.gov/Internet/FSE_DOCUMENTS/fseprd493612.pdf, last visited: Aug 3rd, 2019

- [10] Vetrella, S., Tripodi, C., Colagiovanni, C., & Alfano, A., "Tethered balloons as geostationary platforms for multispectral radiometry". *Acta Astronaut*, 4(5-6), 617-624. 1977
- [11] Klemas, V. "Coastal and environmental remote sensing from unmanned aerial vehicles: An overview". *J Coastal Res*, 31(5), 1260-1267. 2015
- [12] James, M.R., S. Robson. "Mitigating systematic error in topographic models derived from UAV and ground-based image networks." *Earth Surf Proc Land*, 39.10 (2014): 1413-1420.
- [13] Brooks, B.A.; Glennie, C.; Hudnut, K.W.; Ericksen, T., & Hauser, D. Mobile laser scanning applied to the earth sciences. *Eos*, 94(36), 1-3. 2013
- [14] Chen, X., & Vierling, L. "Spectral mixture analyses of hyperspectral data acquired using tethered balloon". *Remote Sens Enviro*, 103(3), 338-350. 2006
- [15] Kushida, K.; Yoshino, K.; Nagano, T., and Ishida, T., "Automated 3D forest surface model extraction from balloon stereo photographs". *Photogramm Eng Rem S*, 75(1), 25-35. 2009
- [16] Pike, D., "Ocean Eye oil spill aerial tracking". *Maritime Journal*, 2014.
- [17] Westoby, M., Brasington, J., Glasser, N., Hambrey, M., Reynolds, J., "Structure-from-Motion photogrammetry: A low-cost, effective tool for geoscience applications". *Geomorphology*, 179, 300-314, 2012
- [18] Li, D., Wrzesien, M., Durand, M., Adam, J. and Lettenmaier, D., "How much runoff originates as snow in the western United States, and how will that change in the future?" *Geophys Res Lett*, 44(12), 6163-6172, 2017.
- [19] Wigmore, O., & Mark, B., "High altitude kite mapping: evaluation of kite aerial photography (KAP) and structure from motion digital elevation models in the Peruvian Andes". *Int J Remote Sens*, 39(15-16), 4995-5015, 2018.
- [20] Koh, L., & Wich, S., "Dawn of drone ecology: low-cost autonomous aerial vehicles for conservation". *Trop Conser Sci*, 5(2), 121-132. 2012
- [21] Mikhail, E.M., Bethel, J.S. and McGlone, J.C., 2001. *Introduction to modern photogrammetry*. New York.
- [22] Nolan, M., Larsen, C., & Sturm, M., "Mapping snow depth from manned aircraft on landscape scales at centimeter resolution using structure from motion photogrammetry", *The Cryosphere*, 9, 1445-1463

ACKNOWLEDGEMENTS AND AFFILIATIONS

This study was supported by CUAHSI Pathfinder Fellowship and the Ohio State University Friends of Orton Hall Scholarship. The authors would like to thank Dennis Lettenmaier for a pre-review of this paper and Ned Bair for his insightful review comments.

Dongyue Li is with the Department of Geography, University of California Los Angeles, CA, 90095 (Email: dongyueli@ucla.edu). Oliver Wigmore and Noah Molotch are with the Institute of Arctic and Alpine Research, University of Colorado Boulder, CO, 80303. Benjamin Vander-Jagt is with the PixElement Inc., OH, 43215. Michael Durand is with the School of Earth Sciences, Ohio State University, OH, 43210. Steven Margulis is with the Department of Civil and Environmental Engineering, University of California Los Angeles, CA, 90095. Roger Bales is with the Sierra Nevada Research Institute, University of California Merced, CA, 95343.

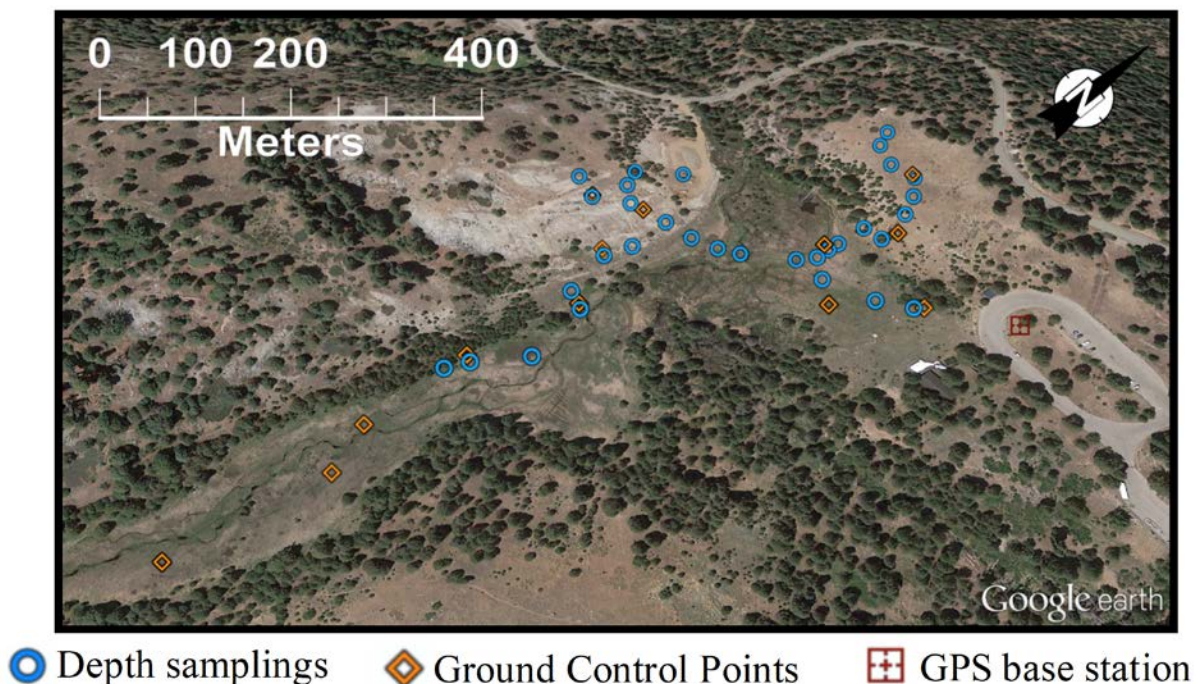


Fig. 1. The Wolverton study site and the position of the ground measurements.

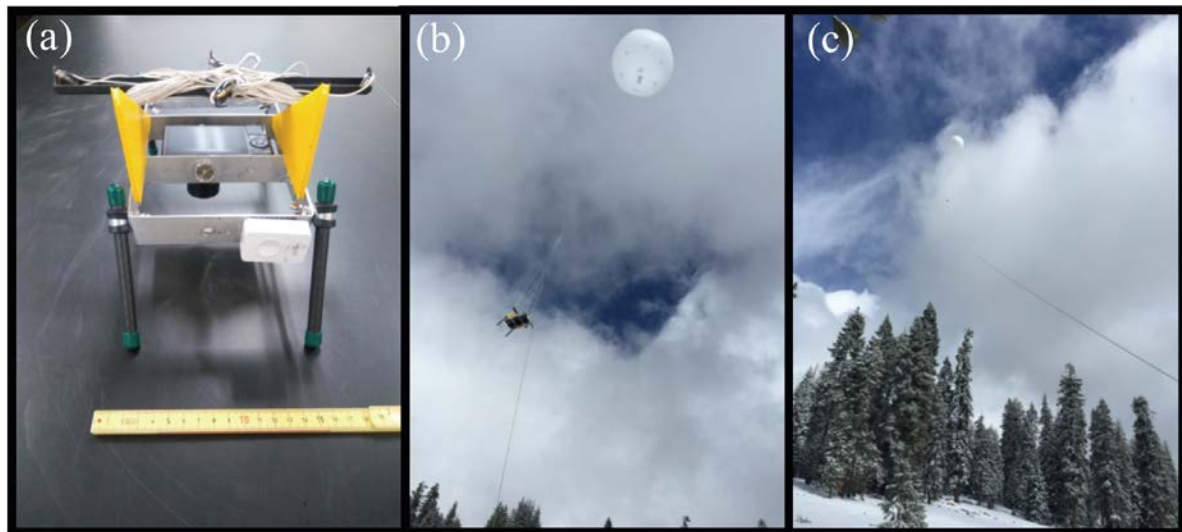


Fig. 2 (a) the rig with the camera, paracord, and the GPS/IMU unit. (b) and (c) show the balloon aerial mapping system in operation.

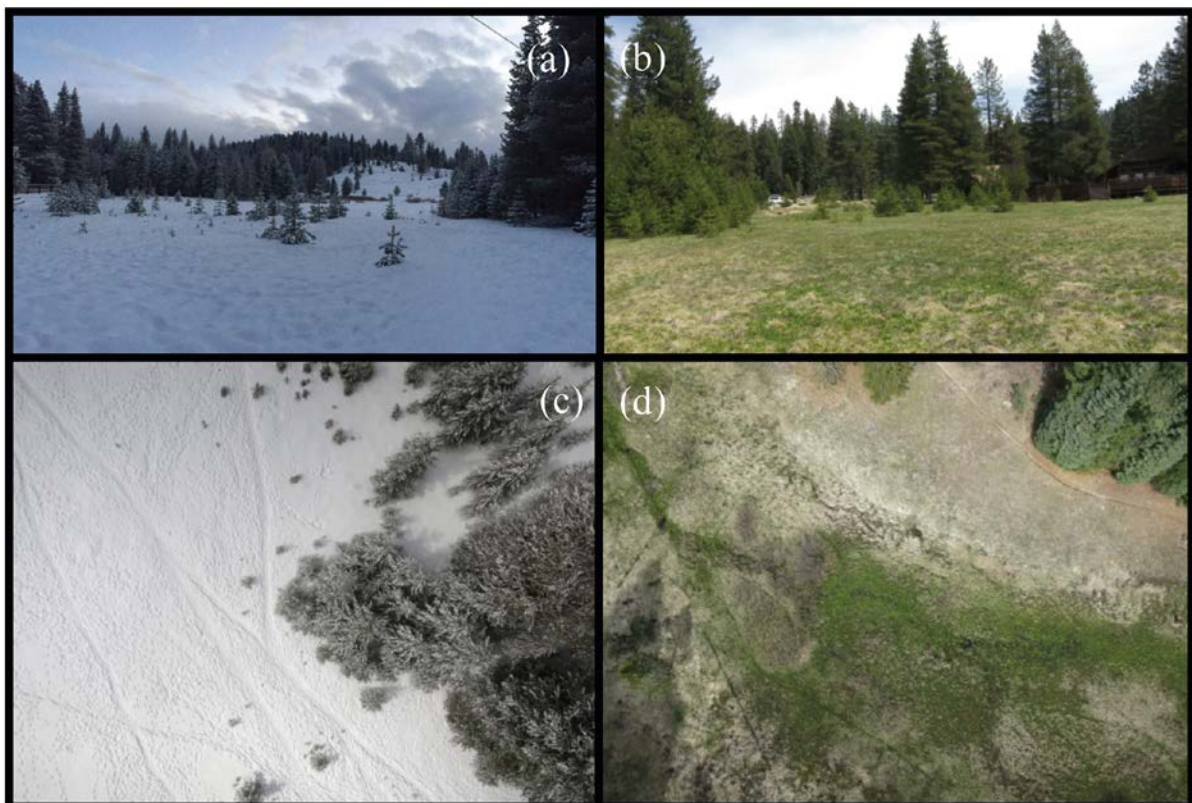


Fig. 3. The study area in the (a) snow-on and (b) snow-off survey, and the sample aerial images taken from the balloon during the (c) snow-on and (d) snow-off survey. Grass had emerged by the time of snow-off survey.

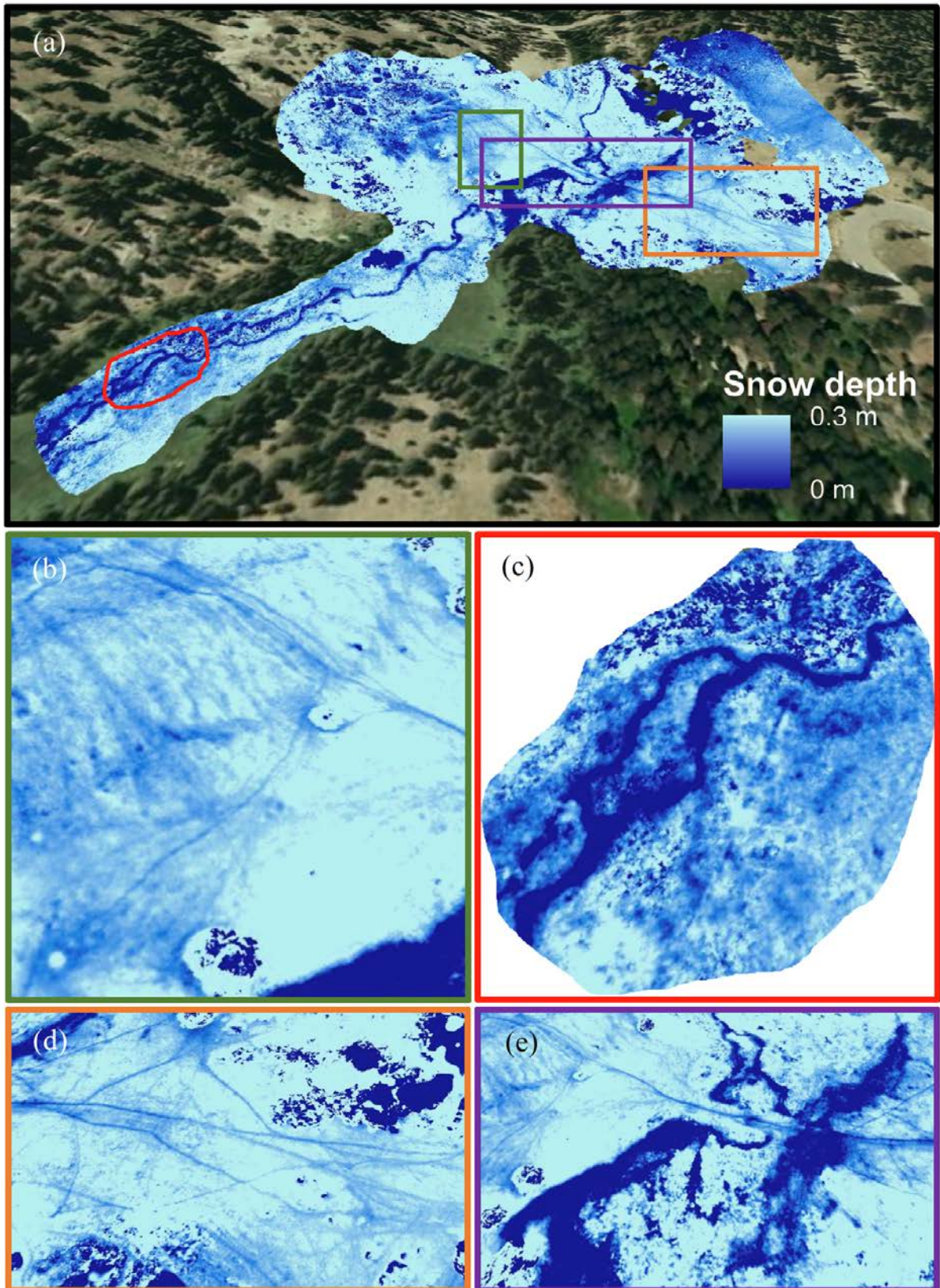


Fig. 4. (a) the photogrammetrically reconstructed snow depth over the survey site. The reconstruction captures the details of the features on the snow: (b) the snow sliding tracks and the two snowballs, (c) the creek meandering, (d) the trails made to facilitate walking, (e) the ponds and the creeks.

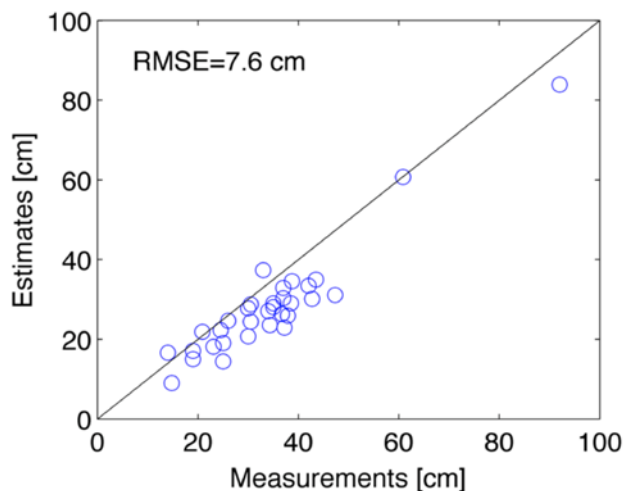


Fig. 5. Comparison between the estimated and the measured snow depth at the depth sampling points.

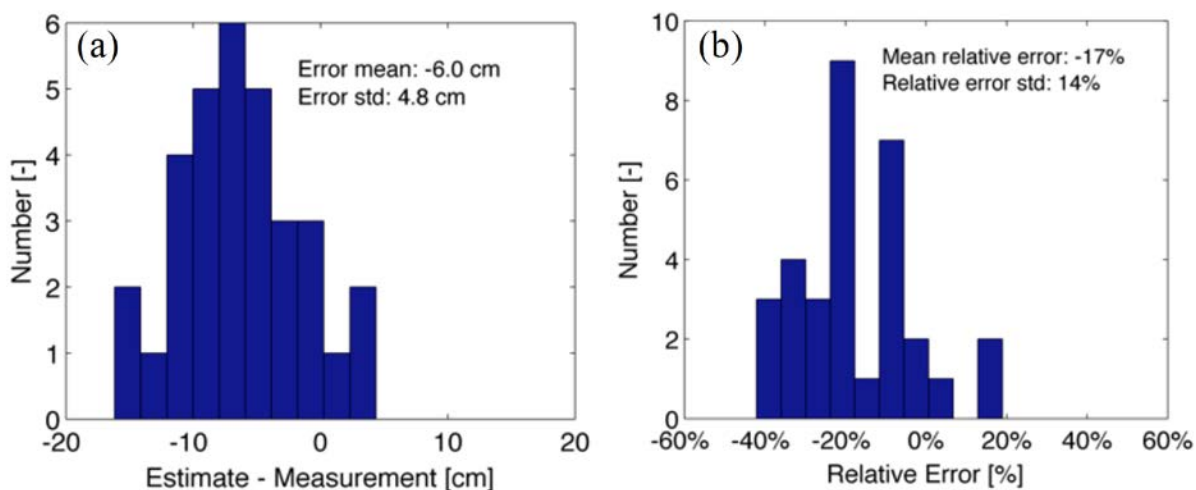


Fig. 6. The histograms showing the distribution of (a) the absolute error and (b) the relative error of the snow depth estimate compared against all the manual depth measurements. The y-axis is the number of the manual depth measuring points where the error falls in each bin of the histogram.

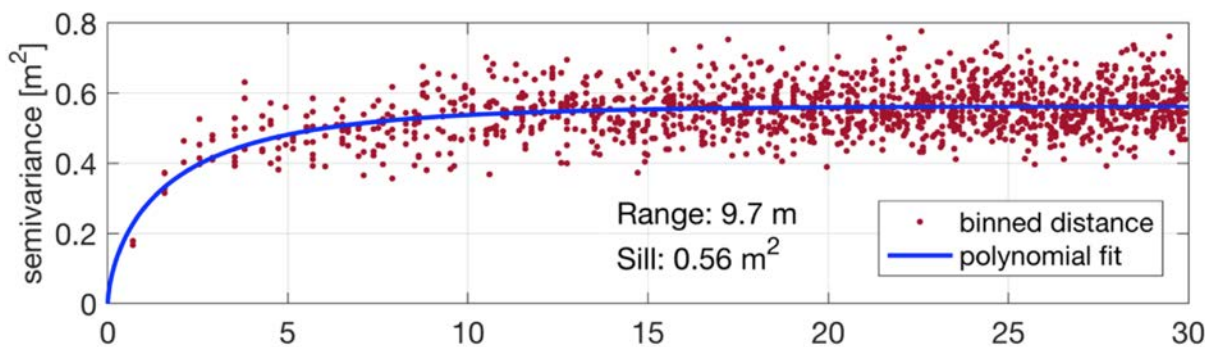


Fig. 7. the semivariogram of the processed snow depth values over the domain. The snow depth reveals significant spatial snow variability at sub-meter scale.